

The SoLi θ experiment @ BR2

New Reconstruction and Calibration techniques

Mykhailo Yeresko^{†,*}

*Laboratoire de Physique de Clermont (UMR 6533), CNRS/IN2P3, Université Clermont Auvergne,
4 Av. Blaise Pascal, F-63178 Aubière Cedex, France*

E-mail: mykhailo.yeresko@clermont.in2p3.fr

The SoLi θ experiment is currently taking physics data close to the BR2 reactor core (SCK•CEN, Belgium), exploring very short baseline anti-neutrino oscillations. It aims to provide a unique and complementary test of the reactor anti-neutrino anomaly by measuring both anti-neutrino rate and energy spectrum. The 1.6 tons detector uses an innovative antineutrino detection technique based on a highly segmented target volume made of PVT cubes and LiF:ZnS phosphor screens. The combination of scintillator signals provides a unique signature in space and time to localise and identify the products of the inverse beta decay to face the high background environment imposed by operating at less than 10 meters from the reactor core without significant overburden. In this contribution we will discuss the technology choices that were made to construct the SoLi θ experiment, the experience gained from its commissioning, calibration, and the detector performance characteristics during three years of non-stop operation. These years of detailed detector characterisation now allow the usage of more sophisticated reconstruction methods, that take better into account the detector's specificities. They will be presented alongside with a new calibration procedure, where the reconstruction of muons allows to measure all relevant detector parameters and where the energy reconstruction and the energy scale are constrained at all relevant scales by a set of calibration sources and control samples from real data (BiPo, and ^{12}B) until high energy with muons.

*41st International Conference on High Energy physics - ICHEP2022
6-13 July, 2022
Bologna, Italy*

*Speaker

[†]For the SoLi θ collaboration.

1. Introduction

The reactor anti-neutrino anomaly has been massively revisited since its first occurrence in 2011[1], although its significance during the last few years is permanently decreasing up to the complete vanishing[2]. Such a behaviour is motivated by the updated nuclear models, latest results from reactor experiments [3] and neutrino observatories [4]. On the other hand, Gallium anomaly along with a “5 MeV bump” remain unexplained[5]. The so-called 3+1 model is within the list of the possible explanations, even with the current tight constraints. It implies the existence of an additional light sterile neutrino state at $\Delta m^2 \sim 1\text{eV}^2$, mixing with the 3 known active neutrinos. According to the model, the largest oscillatory behavior is expected at 2 – 10 meters of traveled distance. Thus, the reactor experiments with a very short baseline are one of the cleanest ways to address the question. Proper event reconstruction and energy calibration are of uttermost importance to ensure the precise flux and energy spectrum measurements.

2. SoLi θ experiment

The Search for Oscillations with a ${}^6\text{Li}$ detector (SoLi θ) experiment belongs to the very short baseline reactor type. The detector is established at the vicinity of the BR2 research reactor (SCK•CEN, Mol, Belgium). This experimental site provides a list of advantages: a very compact core (\varnothing 50 cm) with a unique twisted design, a very short baseline, starting at 6.7 m and 93.5% enriched in ${}^{235}\text{U}$ fuel composition, which simplifies the modeling of the energy spectrum. An employed physics way to detect the anti-neutrino is Inverse Beta Decay (IBD):



The SoLi θ detector relies on the double-scintillation technique in order to track both sources of the signal provided by IBD. It consists of 12800 units, arranged in 50 optically decoupled planes of 16×16 units each. The basic detection cell is a $5 \times 5 \times 5 \text{ cm}^3$ cube of polyvinyl toluene (PVT) plastic scintillator. This hydrogen-rich material is used not only as a target for the anti-neutrino, but also to detect the positron and two subsequent back-to-back annihilation γ s. The high granularity allows to precisely determine the position of the interaction and distinguish the ionisation and annihilation contributions of the positron. Such a feature permits to create a very strong signature of the signal to keep the background at an acceptable level. In addition, each cube is wrapped from two sides with ${}^6\text{LiF}:\text{ZnS}(\text{Ag})$ layers. ${}^6\text{Li}$ is used to capture the thermalized neutron, while the inorganic ZnS scintillator allows to detect the products of the following reaction:



The short prompt part of the signal from the positron (ES) and the long delayed part from the neutron (NS) are correlated with the neutron moderation time (around $65\mu\text{s}$). This complements the signature of the process. The obtained light is transported to the read-out system using wavelength-shifting optical fibres (2 vertical and 2 horizontal in each cube) and converted afterwards into an electrical signal proportional to the number of detected photons by the silicon photo-multipliers (SiPM). This readout information becomes the raw response of the detector.

3. Reconstruction algorithm

The signal candidates, and solely its electromagnetic part, must be defined from the raw response of the detector. In order to get back the list of the impacted cubes and hence employ maximally the high granularity of SoLi δ , the reverse-engineering approach has to be conducted. This is the purpose of the CCube algorithm. The simplified mathematical definition of the reconstruction problem is the following:

$$AE = p, \quad (3)$$

where E is the set of unknown energy contributions, p the values readout by the SiPMs and A is a system matrix (SM) which acts as a projector of the deposited energy to the SiPMs. Each plane is treated as the *separate* problem due to the optical decoupling, ensured with the Tyvek wrapping. The SM has to embody the best knowledge of the detector, for example, the light sharing characteristics (account for the fact that the fraction of received light might escape to the adjacent cubes), differences in the individual features of the cubes, etc. In any case, evaluation of the system matrix with the horizontal muons is discussed in the following subsection. Let's focus here on solving the equation *per se*. It has been widely studied in medical imaging science and lately in high-energy physics [6]. Several different methods were tested including the regularization (FISTA [7]) and Bayesian (Maximum-Likelihood Expectation-Minimization) approaches. The solution obtained by the latter is highly dependent on the initializer. An improved performance is observed, once the preference for the initialisation point is given to the cubes which are at the cross of the fibers having read-out the largest number of photons. It is achieved with the simplified Orthogonal Matched Pursuit (sOMP). Its hybrid with the ML-EM method shows the superior performance for the cube reconstruction efficiency and the rate of fake (so-called "ghost" $\hat{\Omega}$) cubes, while the energy resolution is similar for all the studied approaches. The combination of the sOMP and the ML-EM methods is the current baseline in the SoLi δ experiment.

Method	FISTA	FISTA+ML-EM	sOMP+ML-EM
$\hat{\Omega}$ (%)	15.8	11.4	6.9
ϵ (%)	75.3	76.3	77.7

Table 1: The physics estimators comparison for the considered algorithms.

4. Calibration

The SoLi δ detector is equipped with the automated calibration system (CROSS). It has a carrier for the radioactive sources, which can be placed in 9 positions in 6 gaps between the 5 modules of the detector. The list of available source includes: ^{137}Cs , ^{207}Bi , ^{22}Na , AmBe for the electromagnetic calibration; ^{252}Cf and AmBe for the neutron calibration. The last one employs the waveform-based algorithm to select the pure neutron sample for the calibration. It shows the good agreement between the two available sources. The reconstruction efficiency is measured per cube with an average value of $\epsilon_{\text{Neutron}} = 73.9^{+4.0}_{-3.3}\%$. The calibration campaigns are performed once per several months in

order to secure the consistency of the response over time. The ES calibration relies on the Compton edge fit. Two concurrent approaches are used in the collaboration: Klein-Nishina analytical fit and Kolmogorov-Smirnov test. The developed procedure allows to equalize the SiPMs at 1% level and provides an access to the fibre attenuation and optical coupling. The evaluated results ensures the light yield variation within 5% module per module, estimate the energy resolution at 15% at 1 MeV and test the linearity of the response in the [.5, 4] MeV range. The ES calibration is also performed every several months to track the evolution of the detector response. The outcomes of the NS and ES calibrations with the radioactive sources are summarized in the Figure 1.

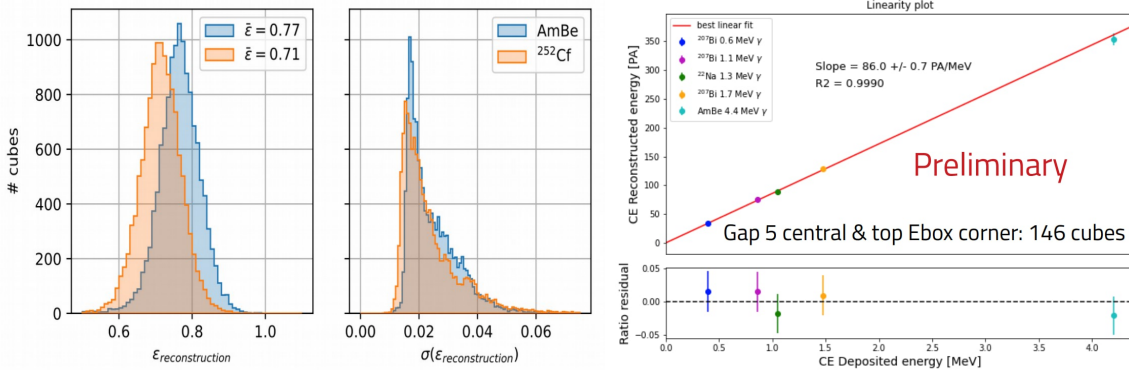


Figure 1: Left: per cube neutron reconstruction efficiency measured with ^{252}Cf and AmBe sources. Right: the linearity plot obtained from the ES calibration in the [.5, 4] MeV range.

4.1 Calibration with horizontal muons

The information, obtained with the radioactive sources, is complemented with a novel calibration procedure with muons. Cosmic muons are a common and practical source of calibration in physics. Selecting horizontal muons (*i.e.* crossing only one cube in the z plane of the detector) can provide even further advantages in the context of the SoLið experiment, since the planes are optically decoupled and hence treated independently. Such that, horizontal muons provide a unique energy contribution addressing the elementary reconstruction (its position is easily identified) and calibration problems. The latter is tackled in two stages.

Firstly, despite the fact the energy source is unique, according to the Figure 2 it does not mean there is a single cube impacted in the plane. That is happening because the scintillation photons are leaking to the neighboring cubes (Light Leakages) and readout by the neighboring fibers in the end. Since muons are depositing about 2 MeV per cm, the LL effect is accurately measured. Overall there are 12 associated light sharing values per cube (4 fibres from the hit cube + 8 fibres from the adjacent cubes). The light sharing is defined equivalently for all of them as:

$$f = \frac{E_{\text{fibre}}}{E_{\text{plane}}} . \quad (4)$$

Thus, there are 12 non-zero values attached to each cube in the SM, which are defined as the result of the fit of the dedicated f distribution. In order to improve the performance of the fit the modified Kullback–Leibler divergence was used. It removes the outliers and make the distribution

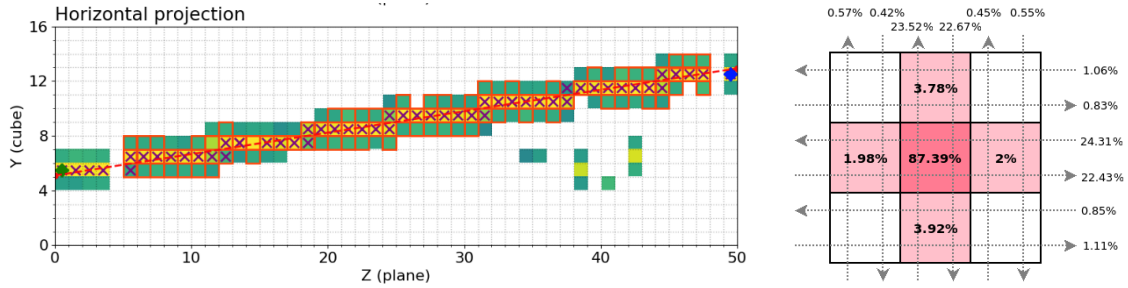
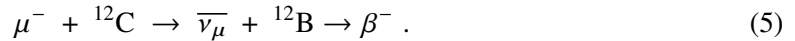


Figure 2: Left: an event display showing the reconstructed track of the horizontal muon from the reactor off data in the y - z plane. Right: Average fractions of the scintillation light distribution between the fibers of the hit cube and the neighboring ones. The results are obtained with the horizontal muon calibration.

more Gaussian. Secondly, to homogenise the response of the detector, the $\frac{dE}{dx}$ distribution is computed for each cube (to do that, the plane energy is complemented with the path length from the muon track fit). The mean values of all distribution are scaled to match the mean $\frac{dE}{dx}$ of the imaginary cube, which includes the $\frac{dE}{dx}$ from all the cubes and all muon tracks considered for the calibration. Such that the individual features of each cube are embodied inside the SM. As for the absolute energy scale the method is flexible, so different references (radioactive sources, average $\frac{dE}{dx}$ expectation value,...) can be used. Finally, the an approach avoids to rely on specific assumptions in the simulation (*e.g.* attenuation). The precision of the calibration is limited by the muon statistics (*e.g.* 10 days are providing 1% stat uncertainty).

The muons can be useful for the validation of the reconstruction and calibration technique as well. For instance, by searching for the cosmogenic background originated from the stopping muon as ^{12}B :



The contamination was identified by searching for the muon, stopped in the detector and an additional ES signal closed in space in time to the end of the track. The ES energy was required to be larger than 3 MeV to reject the background. The remained contamination was statistically subtracted by applying an sPlot technique. The difference in time between the muon and ES ($\Delta t(\text{Muon} - \text{ES})$)

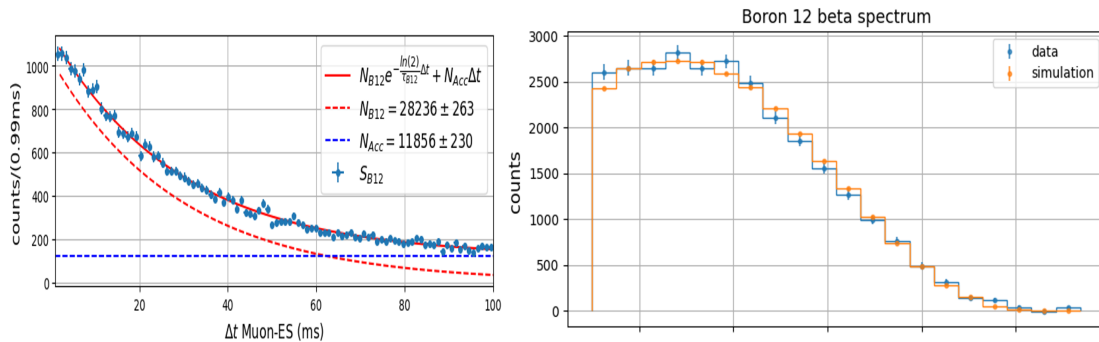


Figure 3: Left: The $\Delta t(\text{Muon} - \text{ES})$ distribution for the ^{12}B candidates with the fit superimposed. Right: the comparison of the subtracted ^{12}B spectrum with the Geant4 simulation prediction.

was considered as the discriminative variable. The Figure 3 shows the result of the fit and the subtracted energy spectrum.

5. Summary and outlook

The novel reconstruction of the EM signal in the SoLi θ detector together with the horizontal muons calibration procedure were presented. The latter ensures the relative calibration of the detector at the 1% level accuracy for the fibres in the main and adjacent cubes, based on the 10 days of the data taking statistics. Hence, the time evolution of the detector response can be tracked more precisely. Several successful cross-checks (*e.g.* identification and reconstruction of the energy spectrum of ^{12}B) provide confidence in the methods employed. Finally, the implementation of the novel methods allows to fully use the high granularity of the detector. It opened new opportunities for the background rejection based on the geometrical topologies analysis (*e.g.* by employing the 2 annihilation γ s signature). They are currently being used to finalise the selection of antineutrino candidates for the Phase I analysis.

References

- [1] T.A. Mueller, D. Lhuillier, M. Fallot, A. Letourneau, S. Cormon, M. Fechner et al., *Improved predictions of reactor antineutrino spectra*, *Phys. Rev. C* **83** (2011) 054615.
- [2] C. Giunti, Y. Li, C. Ternes and Z. Xin, *Reactor antineutrino anomaly in light of recent flux model refinements*, *Physics Letters B* **829** (2022) 137054.
- [3] STEREO collaboration, *Results of STEREO and PROSPECT, and status of sterile neutrino searches*, in *55th Rencontres de Moriond on Electroweak Interactions and Unified Theories*, 5, 2021 [2105.13776].
- [4] ICECUBE COLLABORATION collaboration, *Searching for ev -scale sterile neutrinos with eight years of atmospheric neutrinos at the icecube neutrino telescope*, *Phys. Rev. D* **102** (2020) 052009.
- [5] J.M. Berryman, P. Coloma, P. Huber, T. Schwetz and A. Zhou, *Statistical significance of the sterile-neutrino hypothesis in the context of reactor and gallium data*, *Journal of High Energy Physics* **2022** (2022) .
- [6] A. Simón, P. Ferrario and A. Izmaylov, *Event reconstruction in next using the ml-em algorithm*, *Nuclear and Particle Physics Proceedings* **273-275** (2016) 2624.
- [7] A. Beck and M. Teboulle, *A fast iterative shrinkage-thresholding algorithm for linear inverse problems*, *SIAM Journal on Imaging Sciences* **2** (2009) 183 [<https://doi.org/10.1137/080716542>].